

Supporting information

**SINGLE-CHIP MULTITARGET DETECTION BY
EGOFET-BASED APTASENSOR**

*Elena Yu. Poimanova^a, Elena A. Kretova^a, Anna K. Keshek^{ab}, Askold A. Trul^a, Elena
G. Zavyalova^{ab}, Elena V. Agina^{*ac}*

^aEnikolopov Institute of Synthetic Polymeric Materials of Russian Academy of Sciences,
Profsoyuznaya Str. 70, 117393 Moscow, Russian Federation

^bLomonosov Moscow State University, Chemistry Department, Leninskiye gory 1/3, 119991
Moscow, Russian Federation

^cLomonosov Moscow State University, Department of Fundamental Physical and Chemical
Engineering, Leninskiye Gory 1/51, 119991 Moscow, Russia

e-mail: agina@ispm.ru

Contents

1. Figure S1. The calibration curve for the fluorescently labeled aptamer washed out from EGOFET surface.
2. Figure S2. Transfer characteristics of virus sensors (three devices for example), showing the changes in measurements of EGOFET layers: BTBT-Biotin, Streptavidin, i-motif aptamer BV42, influenza A virus.
3. Figure S3. Target and control measurements transfer characteristics for Influenza A and ND viruses detection by the various aptamer-based EGOFET sensors at different pH: (a) i-motif BV42 aptamer at pH=6, influenza A virus; (b) i-motif BV42 aptamer at pH=7, influenza A virus; (c) i-motif BV42 aptamer at pH=8, influenza A virus; (d) i-motif BV42 aptamer at pH=6, Newcastle disease virus; (e) RBD-1C aptamer at pH=6, influenza A virus; (f) RBD-1C aptamer at pH=6, Newcastle disease virus. Reproducibility of electrical characteristics of EGOFET devices (g). Degradation during consistent measurements of aptamer layer (h).
4. Figure S4. Control measurements transfer characteristics of Newcastle disease virus detection by i-motif aptamer-based EGOFET sensors at pH=6 at different concentrations: (a) 10^5 VP/mL; (b) 10^6 VP/mL; (c) 10^7 VP/mL; (d) 10^8 VP/mL; (e) 10^9 VP/mL.
5. Figure S5. AFM-images and cross-section profiles of EGOFET sensor surfaces (C8BTBTC8/PS – BTBT-Biotin – Streptavidin) with aptamers treated by analytes: (a) BV42 aptamer with influenza A virus, (b) RHA0385 aptamer with influenza A virus, (c) BV42 aptamer after pH measurements, (d) BV42 aptamer after Ag^+ measurements.
6. Figure S6. POM-images of EGOFET sensor surfaces (C8BTBTC8/PS – BTBT-Biotin – Streptavidin) with aptamers treated by analytes: (a) BV42 aptamer with influenza A virus, (b) RHA0385 aptamer with influenza A virus, (c) BV42 aptamer after pH measurements, (d) BV42 aptamer after Ag^+ measurements.
7. Figure S7 - Photograph of the flow chamber applied for multisensory chip testing
8. Figure S8. Transfer curves of the devices operating in saliva (a) and plasma (b) during an hour and a half an hour, correspondingly.
9. Figure S9. Transfer curves of the EGOFET devices modified with the i-motif aptamer and in the presence of target (a, c) and control (b, d) viruses in saliva (a, b) and plasma (c, d).
10. Figure S10 - AFM-images of the EGOFET surface covered by streptavidin layer (a) and by aptamer layer on the top of streptavidin layer (b).

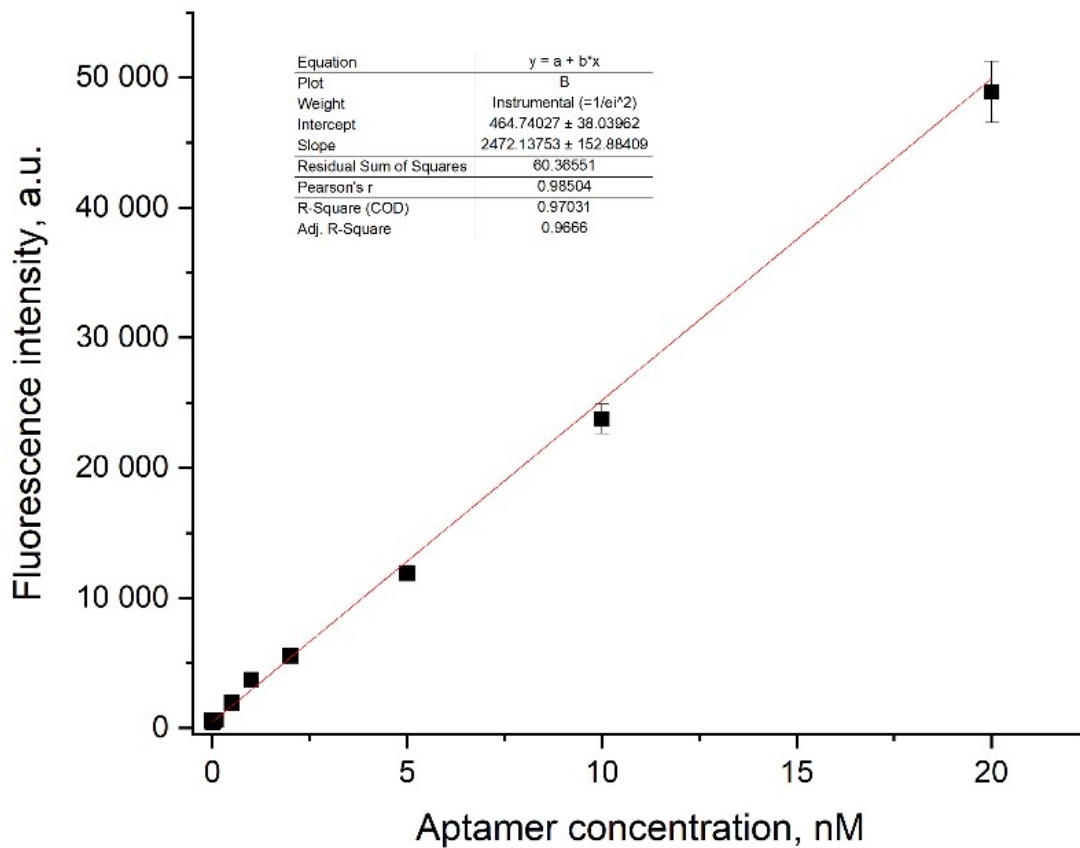


Figure S1. The calibration curve for the fluorescently labeled aptamer washed out from EGOFET surface.

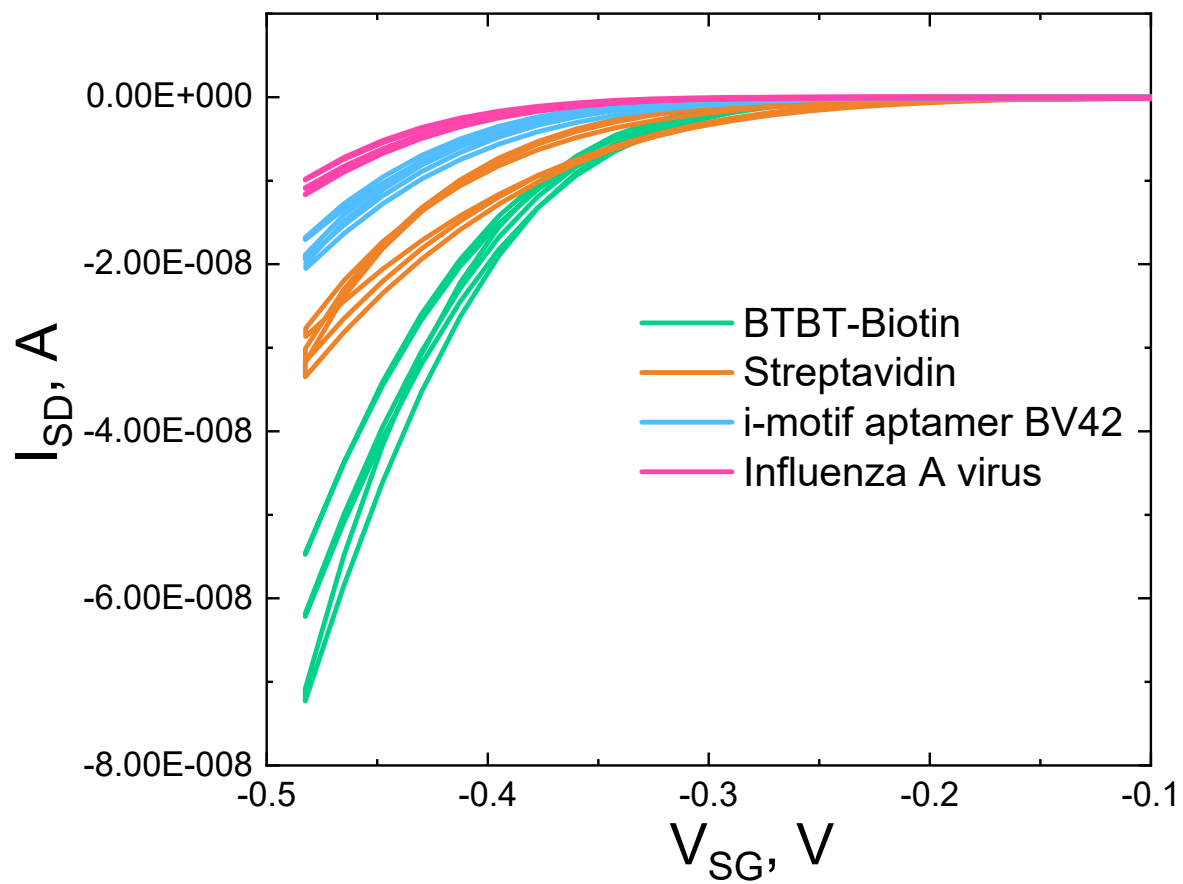


Figure S2. Transfer characteristics of virus sensors (three devices for example), showing the changes in measurements of EGOFET layers: BTBT-Biotin, Streptavidin, i-motif aptamer BV42, influenza A virus.

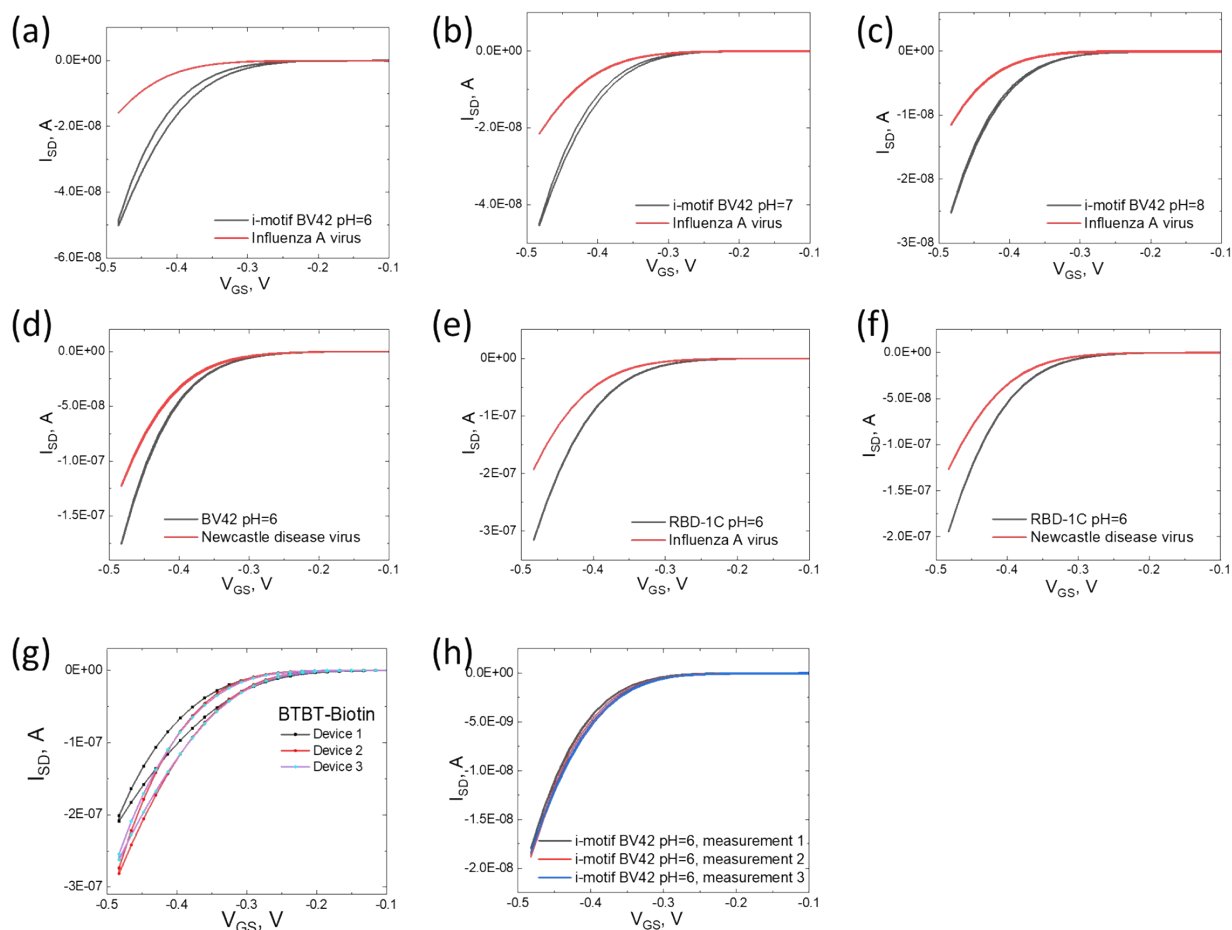


Figure S3. Target and control measurements transfer characteristics for Influenza A and ND viruses detection by the various aptamer-based EGOFET sensors at different pH: (a) i-motif BV42 aptamer at pH=6, influenza A virus; (b) i-motif BV42 aptamer at pH=7, influenza A virus; (c) i-motif BV42 aptamer at pH=8, influenza A virus; (d) i-motif BV42 aptamer at pH=6, Newcastle disease virus; (e) RBD-1C aptamer at pH=6, influenza A virus; (f) RBD-1C aptamer at pH=6, Newcastle disease virus. Reproducibility of electrical characteristics of EGOFET devices (g). Degradation during consistent measurements of aptamer layer (h).

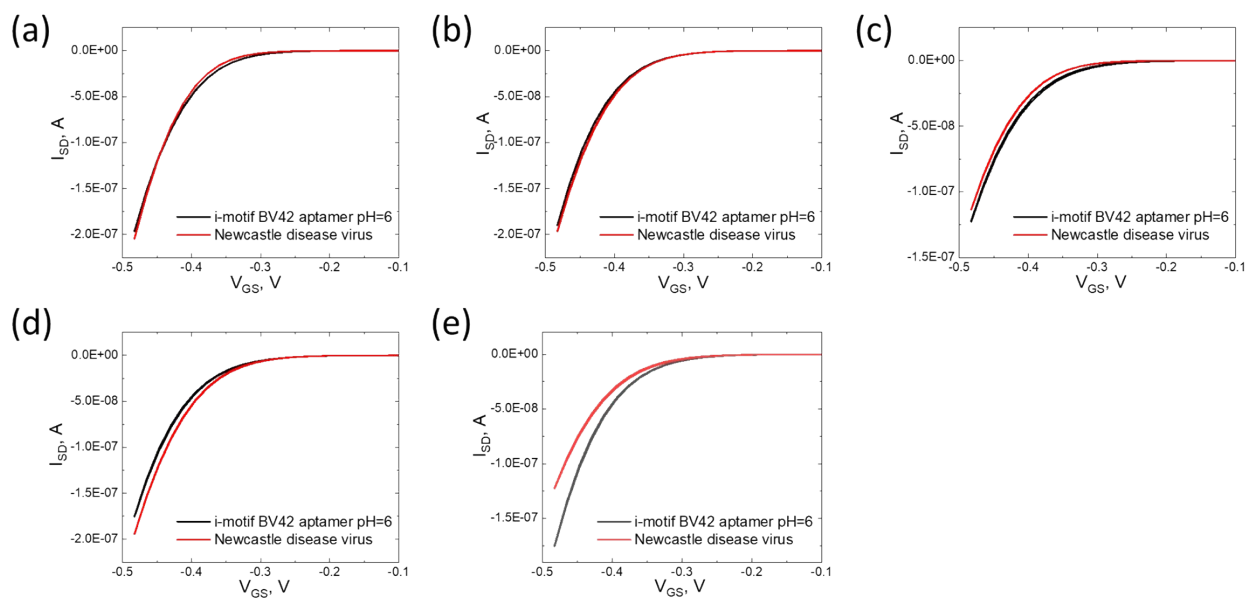


Figure S4. Control measurements transfer characteristics of Newcastle disease virus detection by i-motif aptamer-based EGOFET sensors at pH=6 at different concentrations: (a) 10^5 VP/mL; (b) 10^6 VP/mL; (c) 10^7 VP/mL; (d) 10^8 VP/mL; (e) 10^9 VP/mL.

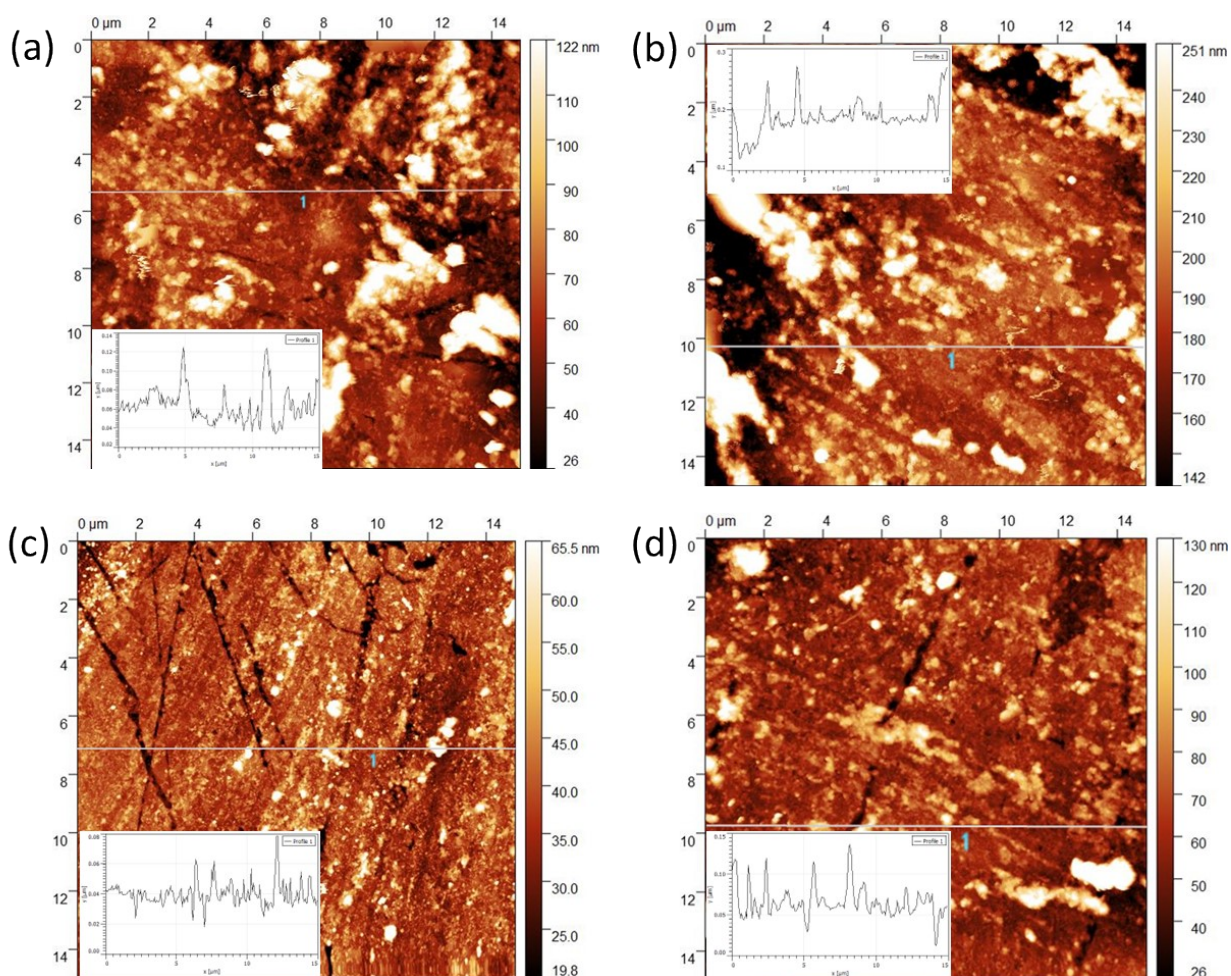


Figure S5. AFM-images and cross-section profiles of EGOFET sensor surfaces (C8BTBTC8/PS – BTBT-Biotin – Streptavidin) with aptamers treated by analytes: (a) BV42 aptamer with influenza A virus, (b) RHA0385 aptamer with influenza A virus, (c) BV42 aptamer after pH measurements, (d) BV42 aptamer after Ag⁺ measurements.

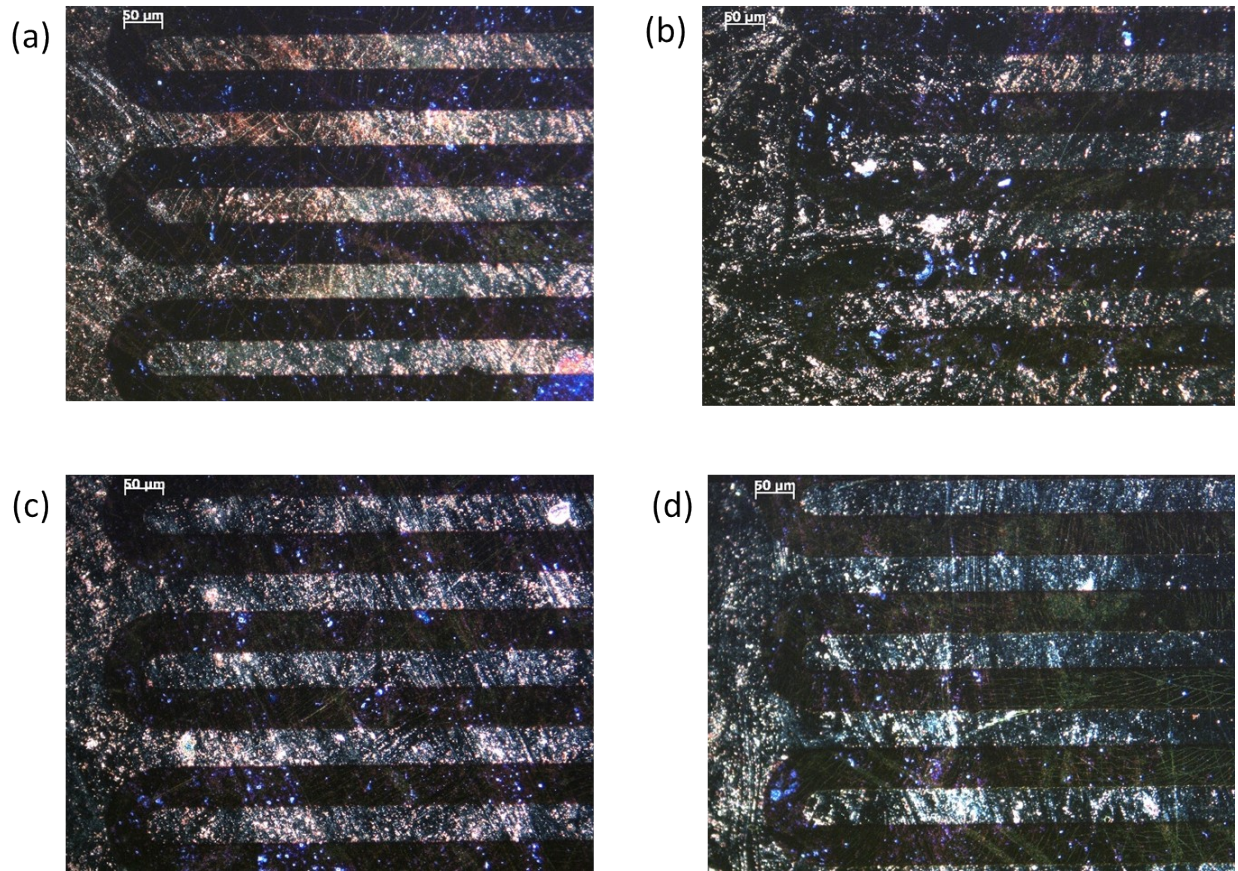


Figure S6. POM-images of EGOFET sensor surfaces (C8BTBTC8/PS – BTBT-Biotin – Streptavidin) with aptamers treated by analytes: (a) BV42 aptamer with influenza A virus, (b) RHA0385 aptamer with influenza A virus, (c) BV42 aptamer after pH measurements, (d) BV42 aptamer after Ag⁺ measurements.

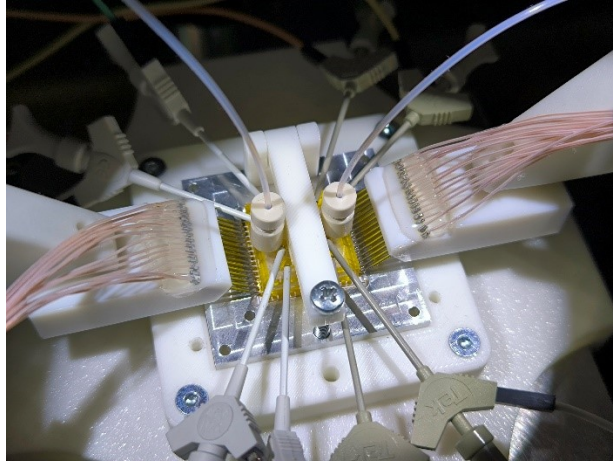


Figure S7 - Photograph of the flow chamber applied for multisensory chip testing

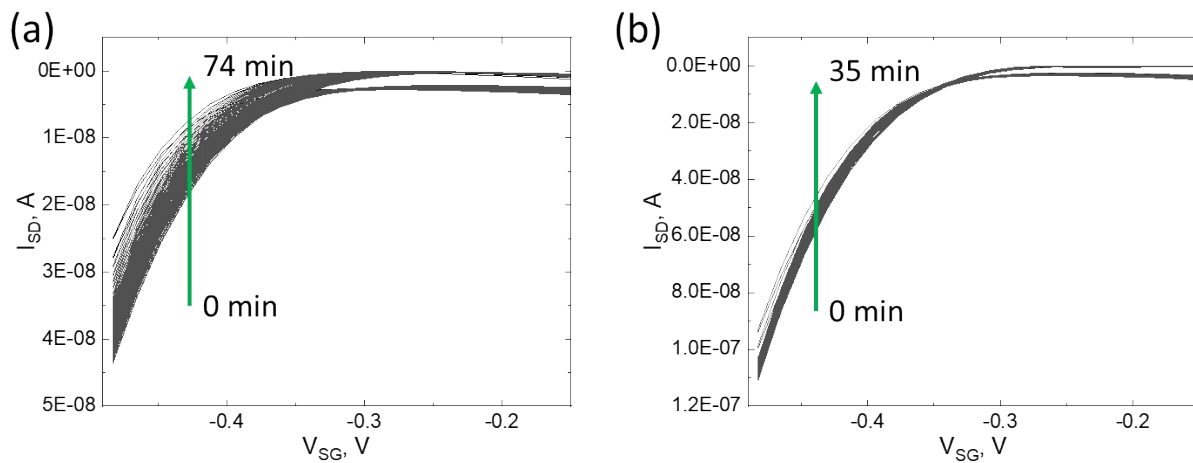


Figure S8. Transfer curves of the devices operating in saliva (a) and plasma (b) during an hour and a half an hour, correspondingly.

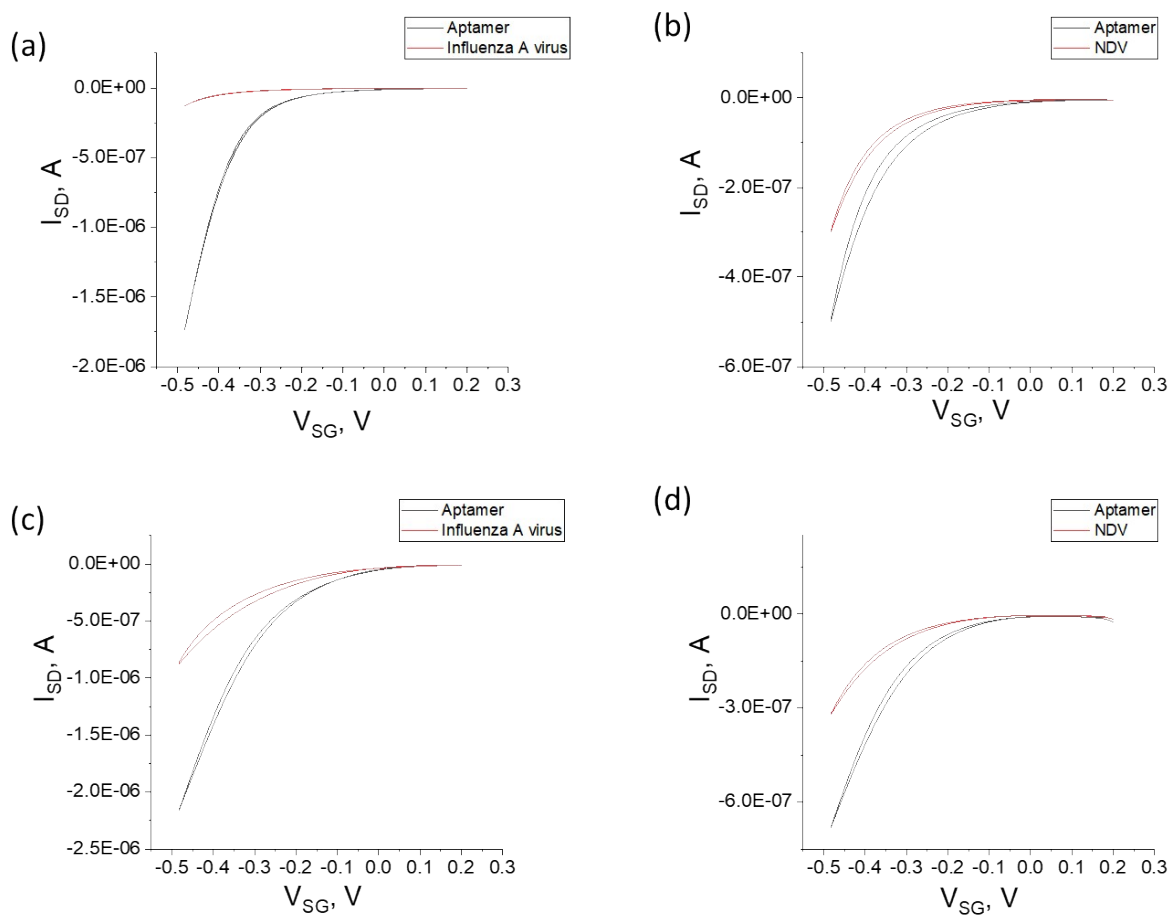


Figure S9. Transfer curves of the EGOFET devices modified with the i-motif aptamer and in the presence of target (a, c) and control (b, d) viruses in saliva (a, b) and plasma (c, d).

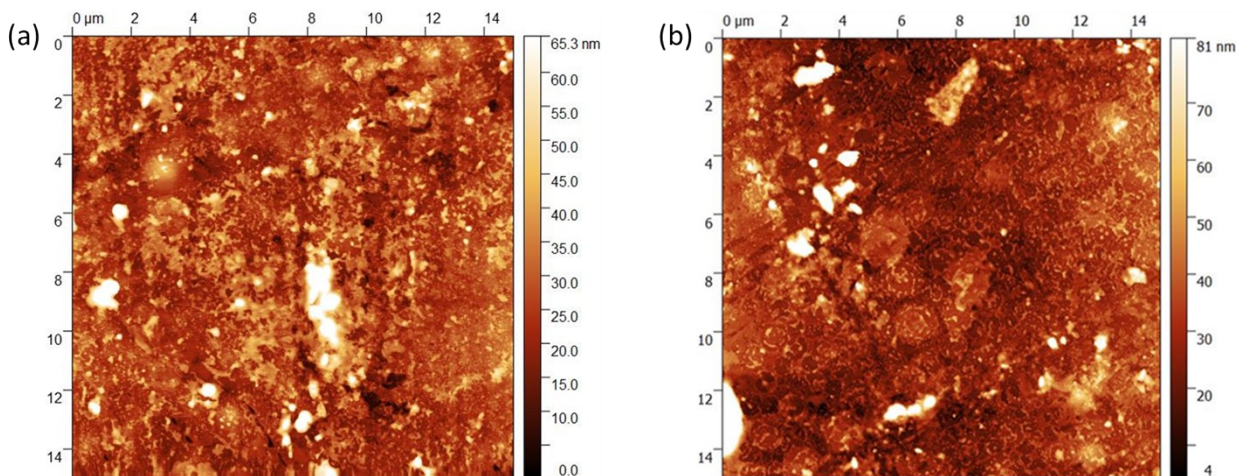


Figure S10 - AFM-images of the EGOFET surface covered by streptavidin layer (a) and by aptamer layer on the top of streptavidin layer (b).”